# Atomic Force Microscopic Analysis of a Porous Membrane with pH-Sensitive Molecular Valves

**Hiroo Iwata, Isao Hirata, and Yoshito Ikada***

*Research Center for Biomedical Engineering, Kyoto University, 53 Kawahara-cho, Shogoin, Sakyo-ku, Kyoto 606, Japan*

*Received August 18, 1997; Revised Manuscript Received March 9, 1998*

ABSTRACT: Much attention has been directed to the development of sophisticated membranes that can regulate the permeability in response to environmental changes. In this study, pH-sensitive membranes were prepared by grafting of poly(acrylic acid) (PAAc) onto a porous Nuclepore membrane. The filtration rate of a membrane with a PAAc graft density of 0.30 $\mu$g/cm$^2$ was 28 times higher at pH 2.4 than at pH 5.4. Atomic force microscopy (AFM) was employed to make clear how the PAAc graft chains regulate the filtration rate. The thickness of PAAc graft layers was determined from the force curve in buffered solutions of various pHs. It was found that the graft layer thickness was several tens of nanometers at pH 2.6 and increased to 20−430 nm at pH 7.6, depending on the PAAc graft density. The PAAc chains grafted on the membrane surface dynamically changed their configuration in response to the medium pH. In addition, AFM images demonstrated that the graft chains shrank and precipitated on the surface of the membrane and the wall of pores at acidic pHs, thereby opening the pores of the membrane, whereas they hydrated and thus effectively closed the pores at neutral and alkaline pHs. The hydrodynamic permeation in conjunction with AFM observation of the graft layers allowed us to conclude that the PAAc graft chains dynamically opened and closed the pores in response to the medium pH, functioning as a molecular valve to regulate the permeation characteristics.

## Introduction

Most of the membranes that play important roles in modern technology are designed in such a way that their permeation properties do not depend on their environment. On the contrary, the membrane of biological cells senses environmental changes and dynamically alters its characteristics in response to the environmental change. Therefore, much attention has been recently directed to the development of more sophisticated membranes that can regulate the permeability in response to environmental changes.[1−3] In previous studies,[1,2] we prepared environment-sensitive membranes by grafting water-soluble polymers on Millipore GVHP 02500 poly(vinylidene fluoride) membranes and found that the grafted membranes varied the filtration rate by several tens of times in response to pH, ionic strength, and temperature. It is very likely that the polymer chains grafted on the membrane surface dynamically altered their configuration in response to the medium change and hence opened and closed the pores like a valve to regulate the filtration rate. At that time we did not have a suitable method to characterize the microfeature of graft chains under a solvated condition. Recently, we used atomic force microscopy (AFM) to characterize a solvated polymer layer grafted on a surface.[4] This AFM technique will allow us to get a deep insight into the dynamic function of the polymer chains grafted on the porous membrane in various media.

In this work, membranes grafted with poly(acrylic acid) (PAAc) to different densities were prepared and AFM was employed to observe the change of graft layer morphology and their thickness at different pHs. The regulation of filtration rate of the membranes in response to pH changes was discussed in conjunction with the dynamic feature of the PAAc graft layer observed by AFM.

* Phone: +81-75-751-4115. Fax: +81-75-751-4144.

## Experimental Section

**Materials.** Nuclepore membranes were purchased from Corning Costar (Acton, MA). The nominal pore diameter, thickness, and membrane diameter were 0.2 $\mu$m, 10 $\mu$m, and 25 mm, respectively. The AAc monomer was purchased from Wako Pure Chemical Industries (Osaka, Japan) and purified by distillation under reduced pressure. Other chemicals were also purchased from Wako Pure Chemical Industries and used as received.

**Grafting of PAAc to Membranes.** To prepare a surface with covalently immobilized polymer chains, graft polymerization of AAc was allowed to initiate from peroxides introduced onto the membrane surface by low-temperature plasma pretreatment, as reported previously.[5] The membrane was treated by Ar plasma under 0.04 Torr for 10 s using a plasma apparatus, Model LCVD12, manufactured by Shimadzu Corp. (Kyoto, Japan). The plasma-treated membrane was immersed in 10 wt % aqueous AAc solution in a glass ampule, which was sealed after vigorous degassing and kept at 60 °C for a given time to decompose the peroxides present on the surface to initiate the AAc graft polymerization. Following graft polymerization, the ungrafted PAAc was removed from the grafted membrane by extraction with deionized water at 60 °C for 1 day. The ungrafted PAAc simultaneously produced during graft polymerization was collected by pouring the solution into acetone and dried under reduced pressure. The degree of polymerization of the graft PAAc chains was assumed to be the same as that of the ungrafted PAAc, which was determined from the intrinsic viscosity in 1 M NaCl by using the following relationship:[6]

$$[\eta] = 9.25 \times 10^{-4} P^{0.9} \quad (1)$$

**Characterization of PAAc-Grafted Membranes.** Morphology of the dried membrane surface was observed by a Hitachi S2380N scanning electron microscope (SEM) under high vacuum. The atomic composition of grafted surfaces was determined by X-ray photoelectron spectroscopy (XPS) using

S0024-9297(97)01243-6 CCC: $15.00 
Published on Web 05/12/1998

**Table 1. Characterization of PAAc-Grafted Nuclepore Membranes**

| membrane code | PAAc grafted[a] ($\mu$g/cm$^2$) | deg of polymzn of the PAAc chain[b] | av area occupied by one PAAc graft chain[c] (nm$^2$) |
|---|---|---|---|
| M-04 | 0.04 | | |
| M-1 | 0.12 | $2.7 \times 10^4$ | $2.7 \times 10^3$ |
| M-3 | 0.30 | $2.9 \times 10^4$ | $1.2 \times 10^3$ |
| M-8 | 0.80 | $2.9 \times 10^4$ | $4.4 \times 10^2$ |

[a] Calculated under the assumption that graft polymerization took place uniformly not only on the membrane surface but also on the wall of the pores. [b] Assumed to be the same as that of the ungrafted PAAc. [c] Calculated from the amount of PAAc grafted per unit area and the molecular weight of the PAAc chain.

**Table 2. X-ray Photoelectron Spectroscopic Analysis of PAAc-Grafted Nuclepore Membranes**

| | $\frac{O_{1s}}{C_{1s}+O_{1s}}$ | $\frac{CH+C{-}O}{CH+C{-}O+OC{=}O+O(CO)O}$ | $\frac{OC{=}O}{CH+C{-}O+OC{=}O+O(CO)O}$ | $\frac{O(CO)O}{CH+C{-}O+OC{=}O+O(CO)O}$ |
|---|---|---|---|---|
| Nuclepore as obtained | 0.17 | 0.93 | | 0.07 |
| polycarbonate | 0.16[a] | 0.94[a] | | 0.06[a] |
| plasma-treatmed nuclepore | 0.20 | 0.85 | 0.06 | 0.09 |
| M-04 | 0.21 | 0.90 | 0.05 | 0.05 |
| M-1 | 0.28 | 0.87 | 0.10 | 0.03 |
| M-3 | 0.28 | 0.85 | 0.13 | 0.02 |
| M-8 | 0.33 | 0.81 | 0.15 | 0.04 |
| PAAc | 0.40[b] | 0.67[b] | 0.33[b] | |

[a] Calculated from the chemical structure of poly(oxycarbonyloxy-1,4-phenyleneisopropylidene-1,4-phenylene). [b] Calculated from the chemical structure of poly(acrylic acid).

ESCA 850V manufactured by Shimadzu Corp. at a pass energy of 1254 eV with a Mg K$\alpha$ X-ray source. The graft density of PAAc chains on the surface was quantitatively determined by the dye-staining method reported elsewhere with slight modification.[7] The dye employed in this study was cationic, toluidine blue O. To stain the grafted membranes, they were immersed in $5 \times 10^{-4}$ M dye solution at pH 10 for 10 h at room temperature. The adsorbed dye molecules were extracted with 8 mL of acetic acid and the amount of PAAc grafted was estimated from the absorbance of the extracted dye solution at 633 nm. Stoichiometric dye sorption with carboxylic groups of PAAc was confirmed using a PAAc gel separately prepared.

**Filtration Studies.** The water filtration rate through grafted membranes was determined under a pressure of 1.0 kgf cm$^{-2}$ using an Amicon 8010 ultrafiltration cell (Bevery, MA) at 25 °C. Buffered solutions were prepared using 0.7 M sodium barbital, 0.7 M sodium acetate, 8.5 wt % sodium chloride, and 0.1 M hydrochloric acid following Michelis' recipe.[8] The solution was agitated by a magnetic stirrer, and the filtrate was collected into a sampling cup at predetermined intervals. The filtration rate was calculated from the weight of the filtrate using the following equation:

$$\text{filtration rate} = \frac{\text{filtrate weight}}{tS} \tag{2}$$

where $S$ is the effective membrane surface area and $t$ is the sampling time interval.

**Characterization of the PAAc-Grafted Layer by AFM.** The AFM apparatus employed in this study was an OLYMPUS NV2000 (OLYMPUS, Tokyo, Japan) with a scanner S30W specialized for AFM observation under water. A PAAc-grafted membrane was fixed by double-sided tape to the cell, immersed in buffered solutions of various pHs in a liquid cell, and analyzed with AFM using a pyramidal probe mounted on a V-shaped cantilever. It was made of silicon nitride with a nominal spring constant of 0.02 N m$^{-1}$. To determine the thickness of the graft layer, deflection of the cantilever was monitored as a function of the height of the sample stage. The thickness of the graft layer was estimated from a force−distance curve derived from the deflection curve of the cantilever using the nominal spring constant, as will be shown in Figure 8. When the surface morphology of the grafted membrane was examined, the force applied on the cantilever was lowered as much as possible to minimize the deformation of the graft layer. The surface was scanned under the tip at a scanning speed of 5.0 $\mu$m/s in the scan direction and 9.8 nm/s in the perpendicular direction. An area of 5 $\mu$m $\times$ 5 $\mu$m was scanned in all cases with 512 $\times$ 512 data points collected per image, which correspond to a data pixel size of 9.8 nm $\times$ 9.8 nm. The buffered solutions were the same as those used in the filtration experiment.

## Results

A Nuclepore membrane, which is an irradiation track polycarbonate membrane with straight cylindrical pores perpendicular to the surface, was used as a substrate membrane for surface graft polymerization of AAc. This membrane offers a much better defined surface and pores to discuss the function of graft polymer chains than Millipore membranes with an irregular open cell form. Similar to previous studies,[1,2] PAAc grafting on the Nuclepore membrane was carried out by Ar plasma activation, followed by graft polymerization of AAc in solution. Four membranes with different graft densities were prepared. The graft density was calculated under the assumption that graft polymerization uniformly proceeded not only on the membrane surface, but also on the wall surface of pores. The graft density of membranes is listed in Table 1. The average area occupied by a single PAAc graft chain was calculated as follows:

$$\text{area occupied by a single graft chain} = \frac{\text{mol wt of PAAc chain}}{\text{graft density}} \tag{3}$$

The calculated areas are also listed in Table 1.

The membrane surface before and after grafting was analyzed with XPS and the observed $C_{1s}$ spectra are shown in Figure 1. The atomic fraction of oxygen and the percentage of each $C_{1s}$ component on the membrane surface are summarized in Table 2. XPS spectra of the untreated Nuclepore membrane are composed of doublet $C_{1s}$ peaks assigned to the hydrocarbon at lower binding energy and to the carbonate O−C(=O)−O carbon at the higher binding energy. Ar treatment caused tailing of the $C_{1s}$ peak at the higher binding energy of the $C_{1s}$ peak around 288 eV. This result suggests that oxygen-containing functional groups such as peroxide and

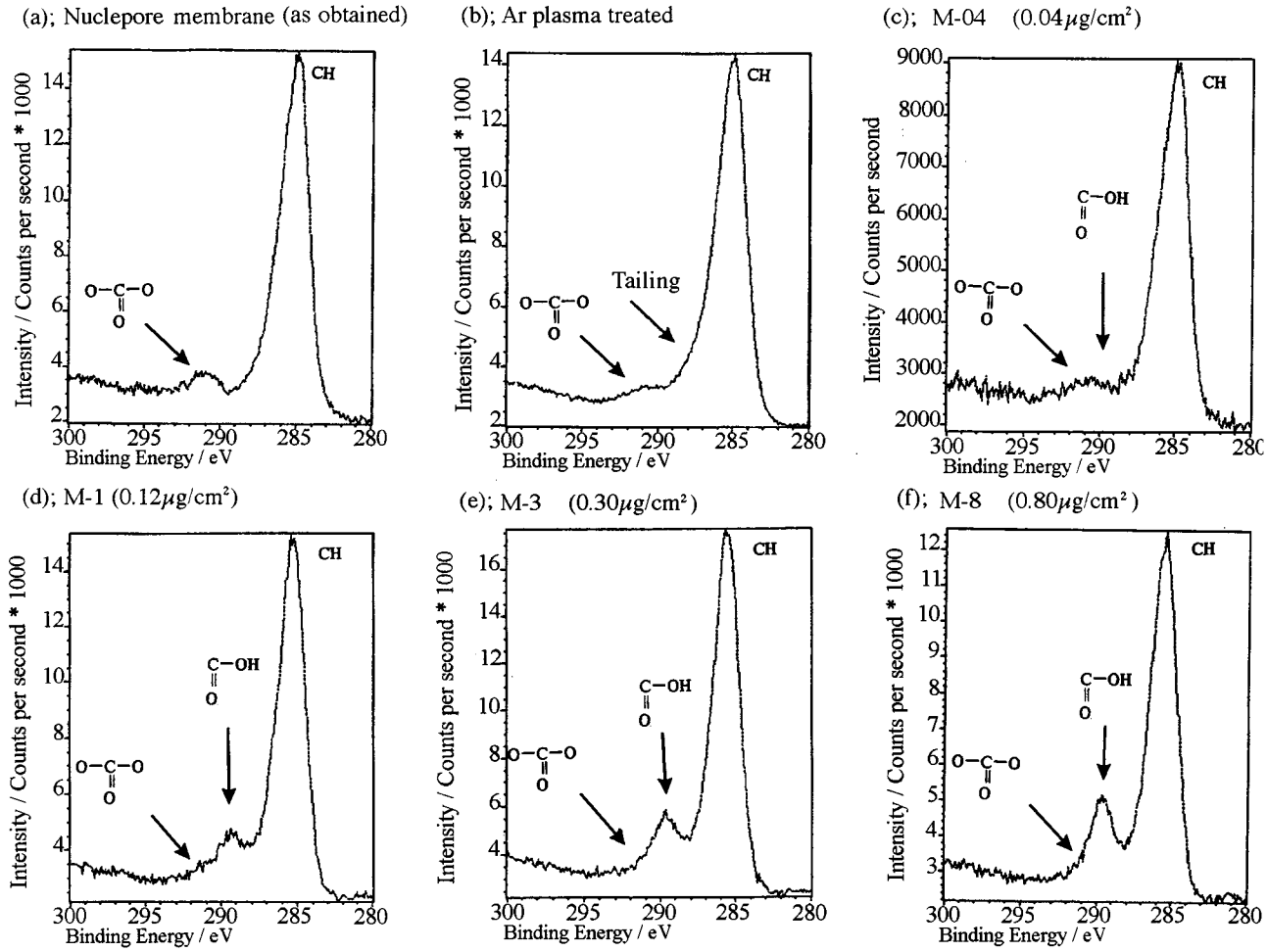


**Figure 1.** X-ray photoelectron $C_{1s}$ spectra of the ungrafted and grafted membrane surfaces.

carbonyl were introduced on the membrane surface. When PAAc chains were grafted onto the membrane, the intensity of the peak corresponding to carbonyl O—C=O increased between the peaks of the hydrocarbon and O—C(=O)—O. The O—C=O peak area became larger as the PAAc graft density increased. These XPS results indicate that PAAc chains are indeed grafted on the membrane surface.

The SEM image of the surface of the ungrafted Nuclepore membrane is shown in Figure 2a. Some defects such as overlapping pores and infrequent dents are observed on the ungrafted Nuclepore surface, but most of the pores have diameters of approximately 0.2 $\mu$m, as specified in the Nuclepore catalog. Figure 2b shows the SEM image of the M-8 membrane, which has the highest graft density of 0.80 $\mu$g/cm$^2$ among the grafted membranes. Even after PAAc grafting, pores are still clearly observed and there is no distinct difference in the pore diameter under the dry state between the ungrafted and the grafted membrane. It is apparent that PAAc grafting did not change the base membrane structure.

The effect of solution pH on the rate of water filtration through the PAAc-grafted membranes is shown in Figures 3and 4. The filtration rate hardly depends on the pH in the neutral and alkaline region. As is obvious, the membranes with graft densities of 0.04, 0.12, and 0.30 $\mu$g/cm$^2$ demonstrate a high dependence of the filtration rate on the solution pH in the acidic region. The filtration rate increases with the decrease of solution pH; for example, the filtration rate of the membrane with the graft density of 0.30 $\mu$g/cm$^2$ is 28 times higher at pH 2.4 than at pH 5.4. The pH region, where the filtration rate sharply increases, shifts to a lower pH in accordance with the increasing graft density of PAAc chains. We did not determine quantitatively the response time of PAAc-grafted membranes to a change of the solution pH, but the membranes could alter their filtration property within a few seconds during exchange of the buffered solution. When a high density of PAAc (0.80 $\mu$g/cm$^2$) was grafted on the membrane, the pH dependence of the filtration rate was hardly observed.

Figure 5 shows representative examples of AFM images of the PAAc-grafted membranes observed in buffered solutions of different pHs. The cantilever easily penetrates into the soft graft layer and hence the AFM image of hydrated PAAc-grafted membranes greatly depends on the force applied to the cantilever. All the AFM images in Figure 5 were recorded under a 1 nN force to minimize the deformation of the water-swollen graft layer (also see Figure 8a). Pores are clearly noticed at pH 2.5, regardless of the graft density. At pH 8.1, all the pores of the M-8 membrane are filled with solvated PAAc graft chains and, in addition, the level of the pore part becomes higher than the other flat region. For the M-3 membrane, pores can be observed still at pH 8.1, but the pores become dim around the rim and more shallow at pH 8.1 than at pH 2.5. PAAc carries a carboxyl group on each side chain, which exhibits various degrees of dissociation depending on the pH of medium. Since the carboxyl group does not dissociate and PAAc chains are precipitated in acidic

(a) Plain Nuclepore membrane as obtained

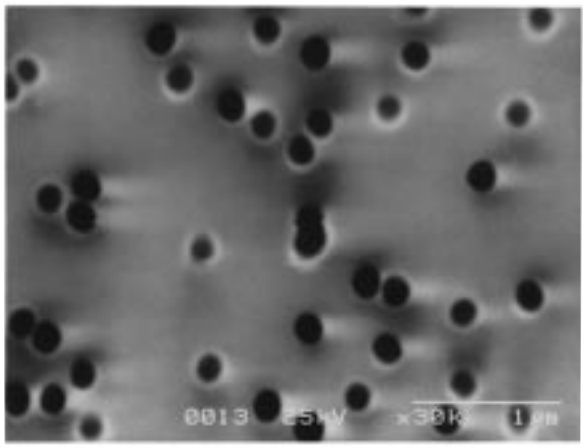

(b) Grafted M-8 membrane (0.80 $\mu$g/cm$^2$)

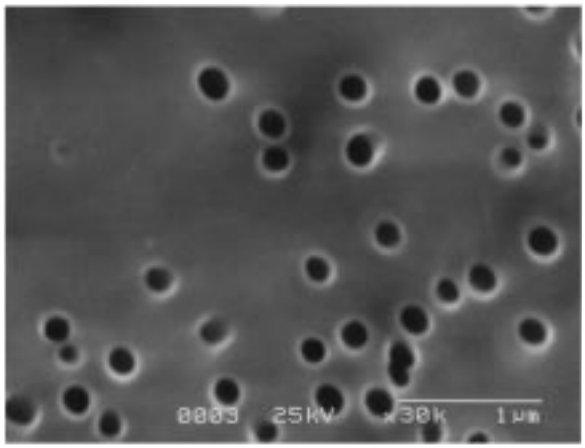

**Figure 2.** Scanning electron microscopic observation of the ungrafted and the grafted membrane (M-8) with the PAAc graft density of 0.80 $\mu$g/cm$^2$.

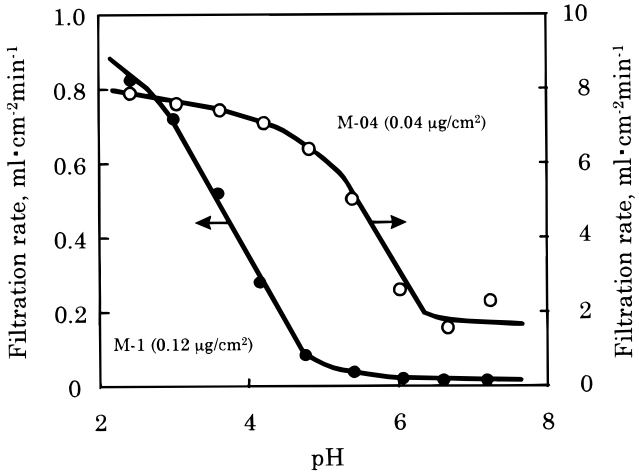


**Figure 3.** pH dependence of the water filtration rate for M-04 and M-1 membranes.

solution, the graft layer is expected to be thin in acidic solution. On the other hand, the carboxyl group dissociates and PAAc is soluble in neutral and alkaline aqueous media. Consequently, the PAAc graft chains will form a highly hydrated soft and thick layer on the membrane surface when polymer chains are brought into contact with neutral and alkaline aqueous media.

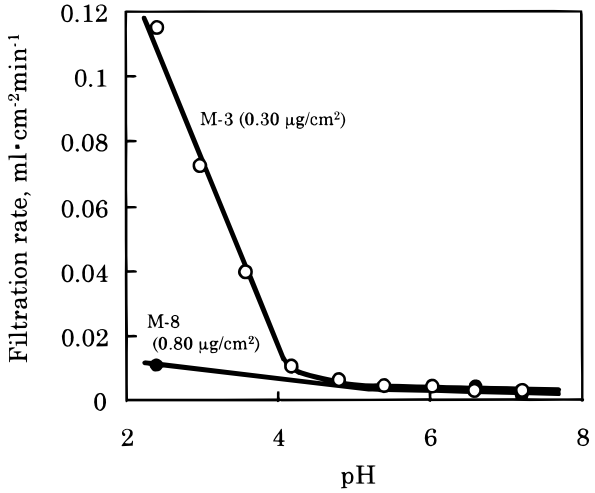


**Figure 4.** pH dependence of the water filtration rate for M-3 and M-8 membranes.

AFM scan lines at and near pores were analyzed to explore the state of the graft chains inside the pores. Figure 6 shows the scan lines of M-3 and M-8 membranes. The scan line at a pore should give a straight well, because the ungrafted membrane has straight cylindrical pores perpendicular to the surface. However, a V shape dent was noticed at the pore. This artifact is definitely due to the interaction of the ridge line of the pyramid-shape probe with the rim of the pore. In fact, the scan line calculated by taking the shape of the probe into consideration, also shown in Figure 6, well reproduced the experimental scan line. Comparison of the experimental with the calculated scan lines gives information about the PAAc graft chains inside the pore. Figure 6b shows the scan lines at and near a pore of the M-3 membrane in various pH media. The scan line at pH 2.5 can be well reproduced by the line curve calculated under the assumption that the scan line was determined by the interaction between the pyramid-shape probe and the rim of the pore. This result suggests that the graft PAAc chains precipitated on the wall of the pore and the pore was opened in acidic solutions. The scan line became more shallow with the increasing pH and thus showed a U shape, suggesting that the pore was filled with the solvated PAAc chains. The M-8 membrane with a higher graft density had a U shape scan line even at pH 2.5, as shown in Figure 6c. The inside of the pore must be filled with precipitated PAAc chains. In the pH region higher than 5, the level of the pore part became higher than the other flat region. Figure 7 shows the dependence of depth or height at the center of pores from the membrane surface on the pH of buffered solution.

The morphological studies mentioned above suggest that the conformational changes of the grafted PAAc chains in various pH solutions determine the pH dependence of the filtration rate. The observation of the graft thickness gives more direct information for the role of the grafted chains in regulating the filtration rate in response to solution pH. The behavior of end-grafted polymer chains in good and poor solvents has been successfully studied by AFM and the surface forces apparatus.[9,10] Overney et al.[9] developed a new ac method, in which a cantilever was approached to the surface by superimposing on the dc approach with a small modulation amplitude, to accurately determine the thickness of the graft polymer layer. However, the

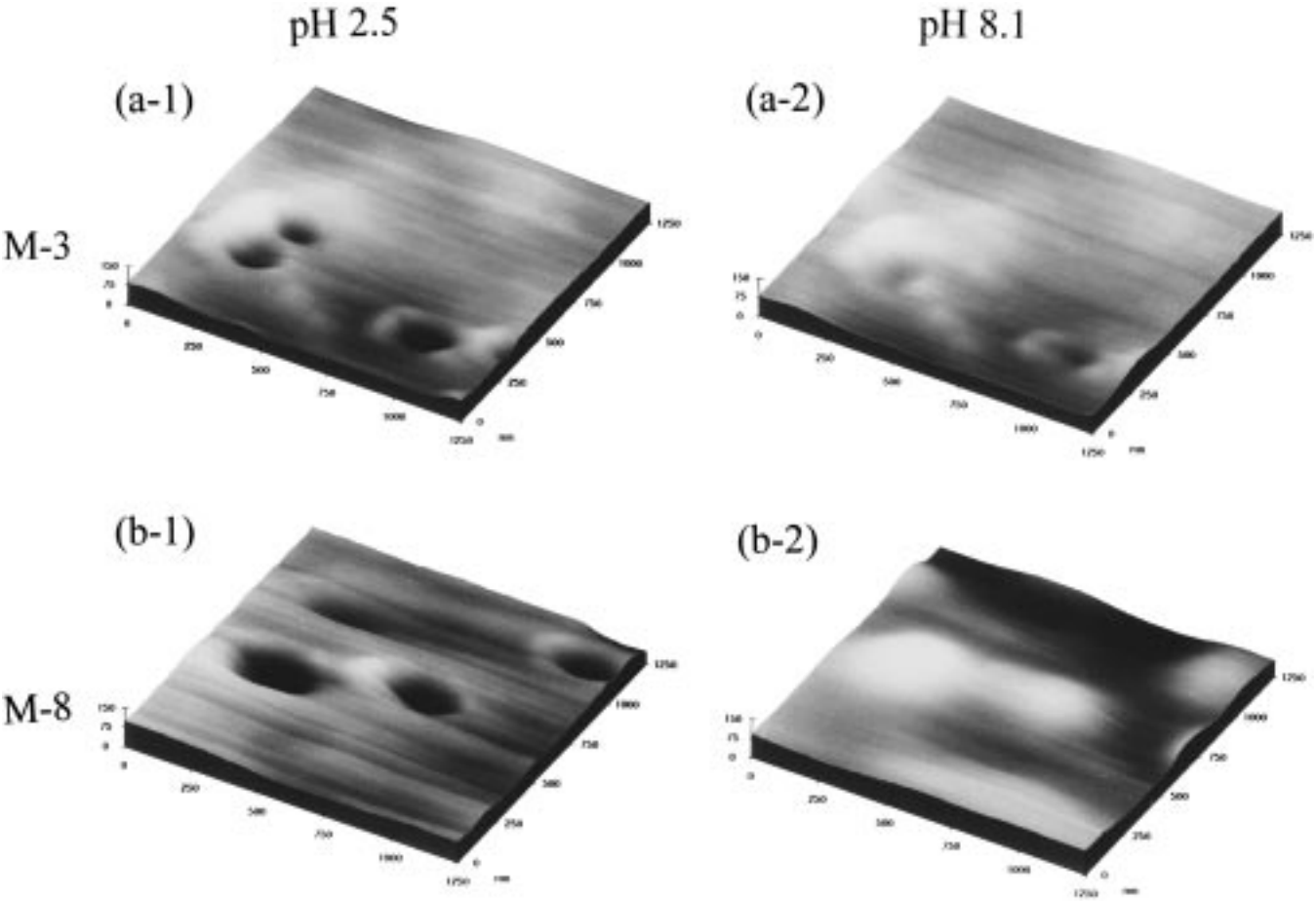


**Figure 5.** AFM images of M-3 and M-8 membranes in buffered solutions of pH 2.5 and 8.1 under 1.0 nN loading on the cantilever.

ac approach could not be performed by our AFM apparatus. The thickness of the graft layer was roughly estimated from the force−distance curve of AFM, as shown in Figure 8. The force−distance curve inflected at the points where the cantilever came in contact with the PAAc-grafted surface and the surface of the substrate membrane, but these points were too dull to determine accurately. To determine the deflection point more accurately, the ratio of an increment of the force, $\Delta F$, to a decrement of the distance, $\Delta z$, was calculated and plotted in Figure 8b. Until the cantilever came in contact with the grafted layer, the ratio, $\Delta F/\Delta z$, was zero. Apparently, $\Delta F/\Delta z$ monotonically increased while the probe penetrated into the graft layer, and then it became a large constant value. The thickness of the PAAc graft layer is assumed to be a distance between the two inflection points of $\alpha$ and $\beta$ indicated in Figure 8b. The thickness of the PAAc graft layer on the grafted membranes is plotted against the pH of buffered solutions in Figure 9. Obviously, the graft layer became thicker with increasing pH. The thickness of the graft layer was 20, 40, 100, and 410 nm at pH 7.6 for M-04, M-1, M-3, and M-8 membranes, respectively. The grafted PAAc chains have expanded conformations that effectively occupy the full space of a 100 nm radius pore.

## Discussion

The graft density and location of graft chains along the membrane cross-section highly depend on the activation method and polymerization condition. For example, a high graft density is attained throughout the cross-sectional region, when the substrate is pretreated with $\gamma$-rays, followed by graft polymerization in the solvent that can swell the substrate.[11] Since the $\gamma$-irradiation grafting makes the substrate larger in size and deformed with the increasing graft density, we have developed a method to restrict the graft polymerization site onto the substrate surface region.[4] If peroxide groups are introduced on the surface region of the substrate at high density and polymerization is carried out in a nonsolvent of the substrate, graft polymerization will be localized at the outermost surface of the substrate. However, the localization of graft chains is uncertain when a porous substrate is used. In this study, graft density was calculated under the assumption that graft polymerization uniformly proceeded not only on the membrane surface but also on the wall surface of pores. If graft polymerization is assumed to be restricted on the membrane surface alone, not on the wall surface of pores, the graft density and the graft layer thickness of the M-8 membrane having the highest graft density became 19.2 $\mu$g/cm$^2$ and 192 nm in the dry state, respectively. This suggests that pores should be closed by the PAAc graft layer even in the dry state. The SEM image, however, showed no distinct difference in the pore size between the nongrafted and the grafted membrane, as shown in Figure 2. These SEM images indicate that the PAAc graft layer not only was localized on the membrane surface but also existed on the wall surface of pores. This is also supported by XPS analysis. If the membrane surface is covered with the PAAc graft layer of 192 nm thickness, the peak originated from the base polycarbonate membrane cannot be observed because the escape depth of photoelectron is approxi-

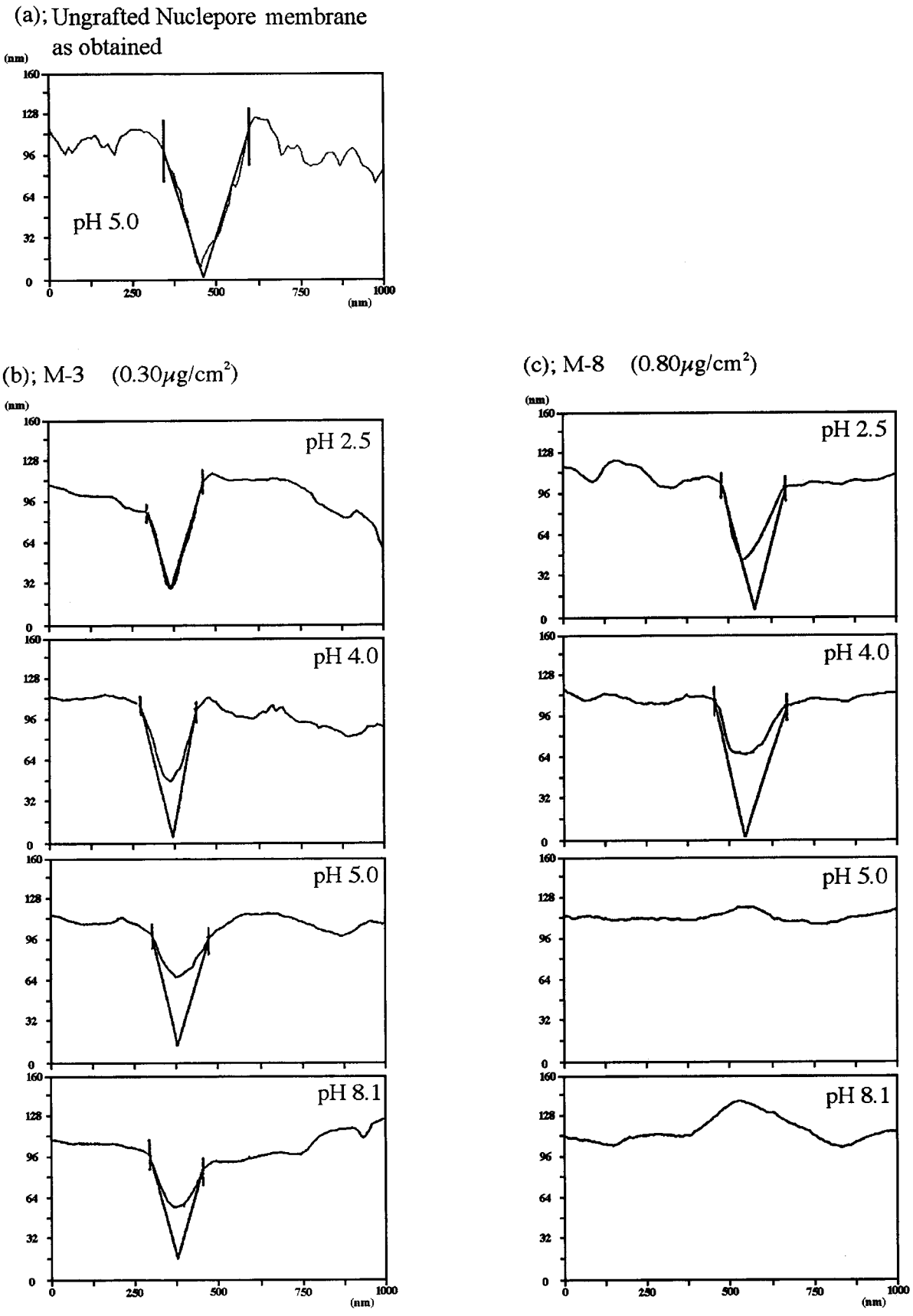


**Figure 6.** AFM scan lines of the ungrafted, M-3, and M-8 membranes at and near a pore.

mately 5 nm.[12] However, the peak of O−C(=O)-O originated from the substrate polycarbonate membrane was observed even on the M-8 membrane and the ratio of the O−C=O peak area to the total area of carbons of M-8 membrane still remained less than that of PAAc.

The thickness of the hydrated graft layer was determined from the AFM force curve and found to highly depend on the pH of the media. PAAc carries on each

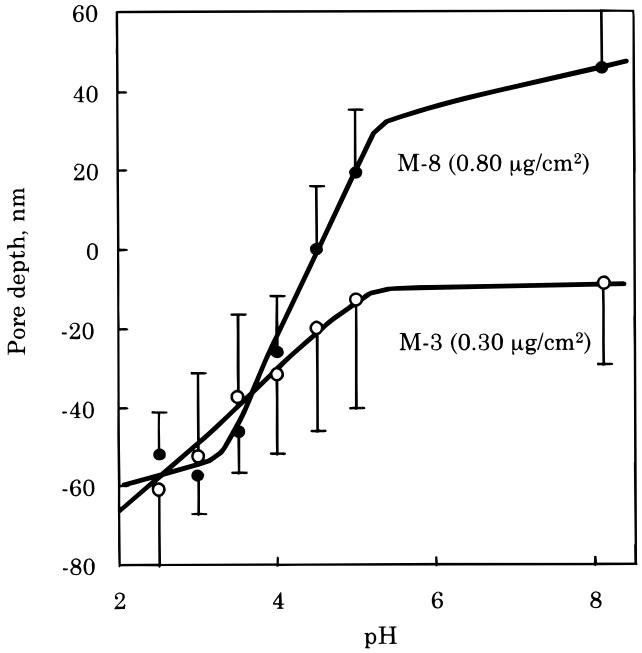


**Figure 7.** pH dependence of the pore depth of M-3 and M-8 membranes on pH under 1.0 nN loading on the cantilever (average and standard deviation of 3−5 times the measurements.)

of the side chains a carboxyl group that dissociates to different extents, depending on the pH of the media. As the carboxylic group does not dissociate in acidic solution, PAAc chains will shrink and be precipitated on the membrane surface and the wall of the pores in the medium of low pH. As shown in Figure 9, the thickness of the graft layer was as thin as several nanometers, while it became thicker in neutral and alkaline media. Although any significant difference in the degree of polymerization of the PAAc was not noted among the PAAc-grafted membranes, the thicknesses of the graft layer highly depended on the graft density. It is well-known that the electrostatic repulsion between not only intramolecular but also intermolecular ionic groups exerts a drastic effect on the solubility and configuration of polyelectrolyte chains.[13] The graft chains carrying dissociated ionic groups have a more expanded configuration. In addition, graft chains with a high surface density are forced to stretch away from the surface by intermolecular interaction, as known in polymer brushes.[14] This effect may induce greater extending and asymmetric conformation to the PAAc chains present on the membrane with higher graft density.

The various AFM images of PAAc-grafted membranes at different pHs can also be explained in terms of configuration of the PAAc graft chains varying in response to pH. The structure of PAAc graft chains near a pore is schematically illustrated in Figure 10, based on the AFM images. In neutral and alkaline solutions, hydrated graft chains effectively close the pores of the membrane, whereas they shrink and are precipitated on the membrane surface and pore wall at acidic pHs. Thus, the graft chains can open and occupy the pores in response to environmental pH change.

The filtration rate depended sharply on the pH of the solution and hence on the thickness of the graft layer. However, it is still questionable whether highly hydrated polymer chains with water contents of approximately 99% can effectively hinder hydrodynamic

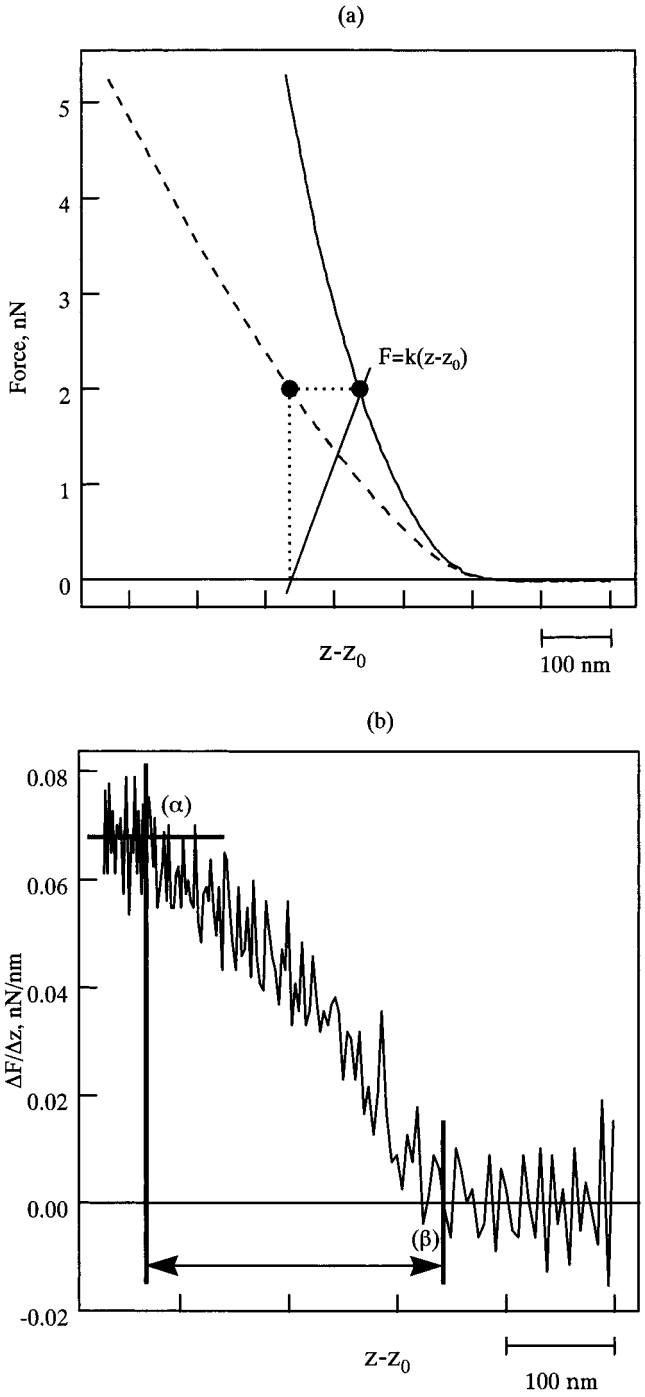


**Figure 8.** Analytical method of a force curve for determining the thickness of the PAAc graft layer. (a) The dotted line is the observed force−distance curve, and the solid line is the force curve corrected by taking the cantilever deflection into consideration using a nominal spring constant of 0.02 N $m^{-1}$. (b) The line indicates the deflection of the interaction force (the thickness of the PAAc graft layer was calculated as a distance between the two inflection points of α and *β*.)

permeation under pressure. As has been fully discussed in respect to the friction properties of polymer molecules in solution,[15] water molecules within a domain of a hydrated polymer chain are mostly immobile even when external pressure is applied, and thus water can move through the area unoccupied by the hydrated polymer chains. The filtration rate through a membrane with cylindrical pores can be expressed by Hagen−Poiseulle's

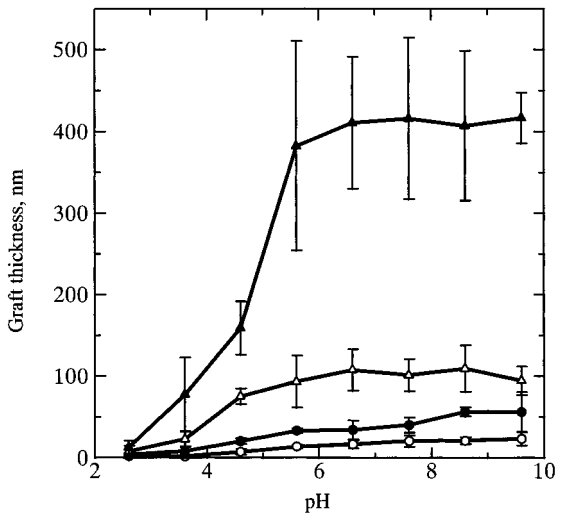


**Figure 9.** pH dependence of the PAAc graft layer thickness (average and standard deviations of five measurements) (bottom to top): (○) M-04 membrane; (●) M-1 membrane; (△) M-3 membrane; (▲) M-8 membrane.

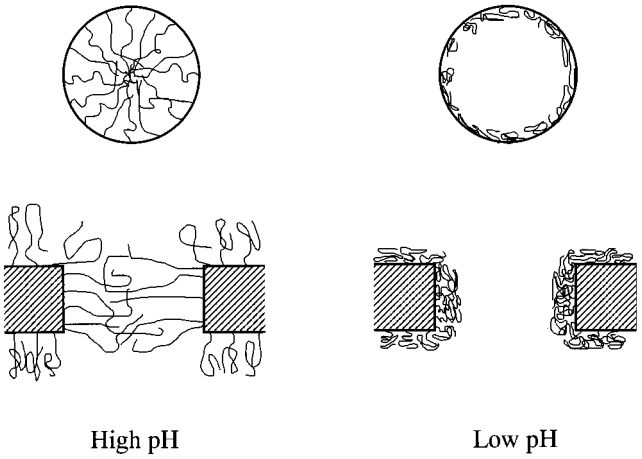


**Figure 10.** Schematic representation of the grafted polymer chains at low and high pHs onto a membrane.

equation as follows:

$$J = \frac{n\pi r^4 p}{8\eta d} \tag{4}$$

where $J$ is the filtration rate, $n$ is the number of pores per unit area, $r$ is the pore radius, $P$ is the applied pressure, $\eta$ is the viscosity of flowing liquid, and $d$ is the length of the capillary or the thickness of the membrane. The dependence of the $J$ value on the fourth power of the pore radius makes the pH dependence of the filtration rate more exaggerated.

Water filtration was studied for four membranes with different graft densities. The M-8 membrane with the graft density of 0.80 $\mu$g/cm$^2$ did not demonstrate a clear pH dependence of the filtration rate. As shown in Figure 6c, the depth line at the pore was U-shaped even at pH 2.5, where the polymer chains might be entangled with each other and thus the inside of the pore should be filled with the precipitated PAAc chains, causing a low filtration rate even in acidic solutions. The other three membranes demonstrated a high dependence of the filtration rate on pH in acidic solutions. The pH region, where the filtration rate sharply increased, shifted to a lower pH in accordance with the increasing density of the PAAc graft chains. The electrostatic repulsion between not only intramolecular but also intermolecular charged groups has a drastic effect on the configuration of polyelectrolyte chains, as discussed above. The intermolecular repulsion force causes the polymer chains attached by one end to a surface at relatively high coverage to stretch away from the surface, forming a polymer brush. This effect becomes more prominent with the increasing graft density of the PAAc chains, as shown in Figure 9. Indeed, the membrane with higher graft density closed the pores more effectively, thereby lowering the filtrate rate even at lower pHs.

In summary, it can be concluded from the pH dependence of the hydrodynamic permeation in conjunction with AFM observation of the graft layer that the graft polymer chains dynamically open and close the pores in response to the pH of the media, acting as a molecular valve to regulate the filtration characteristics.

## References and Notes

(1) Iwata, H.; Matsuda, T. *J. Membr. Sci.* **1988**, *38*, 185.
(2) Iwata, H.; Oodate, M.; Uyama, Y.; Amemiya, H.; Ikada, Y. *J. Membr. Sci.* **1991**, *55*, 119.
(3) Okahata Y.; Noguchi H.; Seki T. *Macromolecules* **1986**, *19*, 493.
(4) Iwata, H.; Hirata, I.; Ikada, Y. *Langmuir* **1997**, *13*, 3063.
(5) Suzuki, M.; Kishida, A.; Iwata, H.; Ikada, Y. *Macromolecules* **1986**, *19*, 1804.
(6) Takahashi, A.; Hayashi, N.; Kagawa, I. *Kogyo Kagaku Zasshi (J. Chem. Soc., Ind. Chem. Sec.)* **1956**, *60*, 1059.
(7) Uchida, E.; Uyama, Y.; Ikada, Y. *Langmuir* **1993**, *9*, 1121.
(8) Chemical Handbook (*Kagaku Binnran Kisohenn II (in Japanese)*); Japanese Chemical Society: 1975; p 1495.
(9) Overney, R. M.; Leta, D. P.; Pictroski, C. F.; Rafailovich, M. H.; Liu, Y.; Quinn, J.; Sokolov, J.; Eisenberg, A.; Overney, G. *Phys. Rev. Lett.* **1996**, *76*, 1272.
(10) Taunton, H. J.; Toprakcioglu, C.; Fetters, L. J.; Klein, J. *Macromolecules* **1990**, *23*, 571.
(11) Chapiro, A. "Radiation Chemistry of Polymeric Systems" *High Polymers*; John Wiley & Sons: New York, 1962; Vol. XV.
(12) Roberts, D. L. *Surf. Interface Anal.* **1980**, *2*, 5.
(13) Oosawa, F. *Polyelectrolytes*; Marcel Dekker: New York, 1971.
(14) Milner, S. T. *Science* **1991**, *251*, 905.
(15) Flory, P. J. *Principles of Polymer Chemistry*; Cornell University Press: Ithaca, NY, 1986; p 606.

MA971243N